An Abiotic Phospholipid Metabolic Network Facilitates Membrane Plasticity in Artificial Cells

Alessandro Fracassi†[1], Andrés Seoane†[1], Roberto J. Brea[2], Neal K. Devaraj[1]*

[1]Department of Chemistry and Biochemistry, University of California, San Diego, 9500 Gilman Drive, La Jolla, California 92093, United States.

[2]Bioinspired Nanochemistry (BioNanoChem) Group, CICA - Centro Interdisciplinar de Química e Bioloxía, Universidade da Coruña, Rúa As Carballeiras, 15701 A Coruña, Spain.

†These authors contributed equally to this work

*Corresponding author. Email: ndevaraj@ucsd.edu

Abstract: The plasticity of living cell membranes relies on complex metabolic networks fueled by cellular energy. Although lipid vesicles have been extensively studied, creating synthetic membranes capable of metabolic cycles remains unrealized. Here we present an abiotic phospholipid metabolic network that generates and maintains dynamic artificial cell membranes. Chemical coupling agents drive the in situ synthesis of transiently stable non-canonical phospholipids, leading to the formation and maintenance of phospholipid membranes. Phospholipid metabolic cycles are capable of driving lipid self-selection and controlling lipid metabolism can induce reversible membrane phase transitions, triggering membrane fusion and lipid mixing. Our work demonstrates that simple lipid metabolic networks can produce artificial cells with lifelike properties, offering insights into mechanisms for engineering synthetic membrane dynamics.

Main Text: Phospholipid membranes serve as barriers, separating cells from the external environment and actively participate in numerous cellular functions such as signaling, transport, and compartmentalization (*1*, *2*). A distinguishing characteristic of lipid membranes is their remarkable plasticity. Cell membranes are robust barriers to small molecules and ions while at the same time are capable of remodeling their composition, shape, and physical properties in response to cellular demands (*3*). The dynamic nature of lipid membranes is due to the presence of numerous specialized metabolic enzymes, which are in turn sustained by the continuous consumption of cellular energy (*4*). Lipid metabolic networks contribute to the plasticity of cell membranes by providing a means for membrane repair, remodeling, and the incorporation of new lipids. For instance, in one part of the phospholipid anabolic pathway, adenosine triphosphate (ATP) and coenzyme A (CoA) are utilized to activate fatty acid precursors, which are coupled to single-chain lysophospholipids to create membrane-forming phospholipids (Fig. 1A) (*5*). Through the catabolic action of phospholipases, phospholipids are continuously disassembled back to lysophospholipids and fatty acid building blocks (*6*), which can once again be activated and reassembled into new phospholipids, completing a metabolic cycle (Fig. 1A). Reconstituted lipid vesicles, while having been useful for elucidating many aspects of natural membrane dynamics, lack the complex metabolic machinery necessary to sustain dynamic processes akin to living cell membranes. As such, there is a need to develop simple strategies that integrate lipid metabolic networks into synthetic membrane systems to generate more lifelike artificial cells.

Here we present an abiotic lipid metabolic network that endows plasticity in artificial cell membranes. In our approach, synthetic derivatives of single-chain lysophospholipids undergo anabolic reactions with in situ activated fatty acids in aqueous environments, leading to the formation of non-canonical diacyl phospholipids that self-assemble into membrane structures resembling cells (Fig. 1B). The resulting chemical linkages are only transiently stable due to hydrolysis, such that catabolism of the lipids occurs over time, returning the starting materials and completing the metabolic cycle. Our study showcases a straightforward synthetic phospholipid metabolic pathway for the generation, maintenance, and remodeling of artificial cell membranes. These metabolically active membranes exhibit several dynamic characteristics reminiscent of natural cell membranes. For instance, the persistence and stability of the formed artificial membranes can be controlled through the supply of chemical activating agents. We demonstrate that multiple rounds of metabolic cycles can promote the preferential selection of specific phospholipids within membranes. Additionally, synthetic phospholipid metabolism can regulate lipid phase transitions and lipid mixing in artificial cells.

The reaction between *N*-hydroxysuccinimide (NHS) and carboxylic acids can be carried out in aqueous media in the presence of an activating agent to produce the corresponding NHS esters, which will hydrolyze over time regenerating both starting materials (*7–10*). While well-known for its application in peptide synthesis (*11*), recently this reaction cycle has been innovatively adapted to transiently mask ionization of carboxylic acids, leading to the formation of assemblies in aqueous media due to the insolubility of the NHS ester generated. Seeking to form more intricate non-canonical phospholipids, we explored the feasibility of utilizing a tailored NHS ester as a linker for tethering two lipid tails together. By employing coupling agents, single-chain NHS-containing lysophospholipids can react with activated single-chain fatty acids, driving the reaction towards the formation of non-canonical diacylphospholipids with the inherent ability to assemble into lipid bilayers. Each lipid contains a labile NHS ester linkage that hydrolyzes with time, but is able to be reformed in the presence of additional activating agent, thus completing an artificial phospholipid metabolic cycle (Fig. 1B).

We began the investigation of such a metabolic cycle by coupling lysophospholipid **1a** and oleic acid **2** to form the 1-oleyl-2-oleyl-*sn*-glycero-3-phosphocholine (DOPC) phospholipid analog **3a** (Fig. 1C). Phospholipid **3a** was generated using standard synthetic methods to verify its ability to form vesicles and determine the optimal hydrolysis conditions for the NHS ester linkage. Upon hydrating phospholipid **3a** in HEPES buffer pH 8.0, micron-sized vesicles were observed by fluorescence microscopy using the membrane-staining dye Texas Red-DHPE (Fig. 1D). Vesicles formed from **3a** could also encapsulate and retain polar molecules such as the dye 8-hydroxypyrene-1,3,6-trisulfonic acid (HPTS) (Fig. 1E). We tested whether phospholipid **3a** could be hydrolyzed back to its precursors and found that at pH 8.0 and 37 °C phospholipid **3a** underwent nearly complete hydrolysis within 24 h (Fig. S4). We also observed formation of 1-oleyl-2-hydroxy-*sn*-glycero-3-phosphocholine (Lyso $C_{18:1}$ PC) as a minor side product, which is due to ester hydrolysis at the *sn2* position (Fig. 2A).

In situ synthesis of phospholipid **3a** from **1a** and **2** was tested in HEPES buffer pH 8.0 using different chemical coupling agents to drive the reaction (Fig. S5). In the absence of enzymes that catalyze its decomposition, ATP demonstrates remarkable stability, remaining intact for hours (*12*). The capacity of ATP to contain a substantial amount of energy while resisting spontaneous decomposition is likely a key reason why ATP evolved as a method for storing and releasing cellular energy. To mimic the function of ATP, the ideal chemical coupling agent must be sufficiently stable during periods of metabolic inactivity, while also possessing the necessary

reactivity for activating fatty-acids (*10*). We screened several candidate agents capable of generating NHS esters (*10*, *13*). For instance, the addition of 1 equivalent of EDC to a mixture of **1a** and **2** in HEPES buffer at pH 8.0 resulted in the formation of phospholipid **3a**, albeit with less than 50% conversion of starting materials to product after 1 h (Fig. S6). We postulated that variations in the solubility of coupling agents, coupled with the presence of precursor lipid assemblies, significantly influenced phospholipid yield. We found that coupling agents with greater hydrophobicity, such as uronium coupling agents, facilitated more efficient phospholipid formation. The use of a uronium salt coupling agent could also help minimize the isomerization of *O*-acylurea to *N*-acylisourea, which has previously led to issues with unreactive *N*-acylisourea accumulating over time (*10*). Notably, complete conversion to phospholipid **3a** was achieved within 15 min upon addition of 1 equivalent of *N,N,N′,N′*-tetramethyl-O-(7-azabenzotriazol-1-yl)uronium hexafluorophosphate (HATU) to a mixture of **1a** and **2** (Fig. 2A, and S7). While HATU may not exhibit the same level of resistance to spontaneous hydrolysis as ATP, it is possible that HATU effectively intercalates within the lipid assemblies, which provides a shield against hydrolysis. We verified that HATU-driven in situ synthesis of phospholipid **3a** led to the generation of phospholipid membranes. Using phase-contrast microscopy, we were able to observe vesicular structures upon the addition of HATU to **1a** and **2** (Fig. S8). The bilayer membrane structure of the assemblies was characterized by cryogenic electron microscopy (cryoEM) (Fig. 2B, and S9).

After establishing conditions conducive to the synthesis and breakdown of phospholipid **3a**, our subsequent aim was to integrate these processes to achieve successive cycles of phospholipid **3a** formation (anabolism) and hydrolysis (catabolism). To this end, we introduced 1 equivalent of HATU to a mixture of **1a** and **2** in HEPES buffer at pH 8.0, resulting in near quantitative formation of phospholipid **3a**. Following a 24 h incubation at 37 °C, phospholipid **3a** underwent hydrolysis back to its precursors. This cycle was repeated three times, with each iteration demonstrating conversion of **1a** to **3a** (Fig. 2C). We observed a decrease in the total concentration of phospholipid **3a** after each cycle, primarily attributed to the formation of the Lyso $C_{18:1}$ PC side product during hydrolysis (Fig. 2A).

Cells rely on cellular energy to maintain and remodel the structures of their lipid membranes (*5*, *14*). Despite the continuous turnover of phospholipids, the overall structural integrity of cellular membranes remains intact, ensuring the containment of internal aqueous content without leakage. Similarly, in our system, continuous addition of coupling agents sustains the persistence of intact synthetic phospholipid membranes by maintaining the metabolic network. We encapsulated a polar fluorescent dye within the vesicles of phospholipid **3a** such that, if sufficient phospholipid **3a** were to be broken down, there would be a loss of membrane integrity, and encapsulated dye would be released into the surrounding environment. Phospholipid vesicles composed of **3a** were formed with encapsulated Cy5 dye (Fig. 2E). We split the vesicle sample into two portions, with only one half receiving 1 equivalent of HATU coupling agent. Both mixtures were then incubated at 37 °C for 24 h and analyzed by spinning-disk confocal microscopy. In the absence of any coupling agent, catabolism took place, phospholipid **3a** hydrolyzed, and complete release of the dye contents was evident (Fig. 2D). However, vesicles exposed to HATU were persistent and retained the encapsulated Cy5 indicating their membrane structural integrity was preserved. Thus, by providing HATU as chemical energy to sustain phospholipid metabolism, the ongoing hydrolysis of phospholipid **3a** was swiftly reversed through recoupling, ensuring both vesicle integrity and retention of the dye within (Fig. 2D).

Unexpectedly, we noticed that the addition of coupling agents to membranes of **3a**, not only preserved the structural integrity of the phospholipid vesicles, but also suppressed the formation of the hydrolysis side product Lyso $C_{18:1}$ PC. We examined side product formation under identical conditions for samples of precursor **1a** alone, **1a** in the presence of **2**, phospholipid **3a** alone, and **3a** with the addition of 1.5 equivalents of HATU every 24 h. Upon incubation at 37 °C for 48 h, HPLC-MS-ELSD results showed that samples lacking HATU accumulated a significant and comparable level of side product, whereas the addition of HATU to sustain the metabolic network resulted in the formation of only trace amounts of side product (Fig. S10). This observation is in line with prior studies indicating that phospholipid hydrolysis may be influenced by factors such as the state of aggregation and membrane packing (*15*). To further explore how HATU affects lipid side product formation, we created a dispersion containing **1a** and **2**, to which we added 1 equivalent of HATU, resulting in conversion to phospholipid **3a**. Subsequently, we divided the sample in two portions. The first half received an additional equivalent of HATU and was incubated at 37 °C for 48 h. In contrast, the second half was directly incubated at 37 °C and, with the second equivalent of HATU added only after 24 h, when hydrolysis of **3a** occurred. We waited an additional 24 h incubation period at 37 °C and analyzed both halves by HPLC-MS-ELSD. Thus, both halves of the initial sample had been treated with a total of 2 equivalents of HATU over 48 h and were incubated for the same amount of time at 37 °C. Upon analysis by HPLC-MS-ELSD, we observed that the sample to which excess HATU was added all together displayed minimal formation of side product, while the system subjected to complete hydrolysis showed a considerable higher amount of Lyso $C_{18:1}$ PC side product (Fig. S11). Thus, maintaining lipid membrane stability by providing excess HATU appears to inhibit unproductive side reactions, effectively slowing down system deterioration. This finding highlights an interesting analogy with natural systems, where the continuous provision of energy is required to maintain membrane integrity, averting side reactions and ultimately preventing cell death.

Biological membranes undergo continuous remodeling of their lipid composition through lipid metabolism. It is unclear whether simplified abiotic artificial membranes can achieve analogous compositional remodeling. This question holds significance for both the evolution of artificial cells and protocellular behavior at the origin of life. In principle, persistent metabolic remodeling of lipids could lead to the selection of membranes that confer better fitness to artificial cells (*16*, *17*). In our system, such molecular self-selection might be achieved through the generation of assemblies of differing hydrolytic stability. As a consequence of the increased tendency of hydrophobic molecules to remain shielded in the assembly, the kinetics of the deactivating hydrolysis reactions would be expected to vary among different lipid species based on lipid polarity. Previous studies have demonstrated that repeated rounds of acylation and hydrolysis could promote the self-selection of prebiotically relevant lipids (*18*). However, in these experiments, activated precursors were synthesized independently and then introduced into the system for each acylation cycle. Additionally, the hydrolysis step necessitated higher temperatures of up to 70 °C and a basic pH.

To assess whether our abiotic phospholipid metabolic network could facilitate the enrichment of specific phospholipid types in artificial cell membranes (Fig. 3A), we synthesized two NHS-containing lysophospholipid precursors with varying alkyl tail lengths, designated as **1b** and **1c**. We expected that the hydrolysis rate of the phospholipids obtained by conjugating either **1b** or **1c** with compound **2** to form **3b** or **3c** respectively, would vary significantly, with faster hydrolysis expected for **3c** due to its shorter alkyl tails. By using HPLC-MS-ELSD to monitor the hydrolysis of **3b** and **3c** in HEPES buffer pH 8.0 at 25 °C, we determined that **3c** hydrolyzed almost completely within 48 h, while nearly 60% of **3b** remained intact (Fig. S13). Subsequently, we

prepared a mixture containing 1 equivalent each of lysophospholipid **1b** and **1c**, along with 1 equivalent of oleic acid **2** as a limiting reagent. The addition of 1 equivalent of HATU resulted in the rapid formation of **3b** and **3c** in an approximate ratio of 1:1 with consumption of **2**. After incubating the sample for 48 h at room temperature, **3c** was almost fully hydrolyzed while **3b** remained stable. The coupling/hydrolysis cycle was repeated 3 times, calculating the amount of added HATU based on the oleic acid **2** that was free for reaction. Remarkably, we observed a progressive increase in the ratio of **3b/3c**, shifting from 1:1 initially to nearly 2:1 by the end of four metabolic cycles (Fig. 3B). The observed shift in phospholipid ratio across the cycles demonstrates the ability of the membranes to remodel and undergo phospholipid self-selection, illustrating the utility of having metabolic cycles in artificial cell membranes, despite the need for constant input of chemical activating agents.

Living cell lipid membranes exhibit diverse shapes and morphologies, crucial for various biological functions. While cellular membranes are predominantly composed of lamellar structures, nonlamellar phases also play important roles in segregating biomolecules, facilitating biochemical reactions, and creating unique local architectures for membrane fission and fusion (*19–21*). Under specific conditions, certain subcellular compartments undergo structural transformation from lamellar to nonlamellar phases. For instance, during germination, etioplasts in plant cells transition from lamellar to nonlamellar membranes upon exposure to light (*22*, *23*). Despite previous investigations on the utilization of nonlamellar lipid phases in artificial cells (*24–31*), the precise control of phase transitions within these systems remains a significant challenge (*32–35*).

Regulating phospholipid formation might be used to trigger phase changes in mixed lipid assemblies. It has been shown that lipid nonlamellar phases are tolerant to the presence of diacyl phospholipids. However, single-chain precursors such as lysophospholipids and fatty acids, can disrupt the stability of nonlamellar phases and trigger transformation to lamellar phases (*36–38*). We hypothesized that a phospholipid metabolic cycle might serve as a mechanism to regulate lipid phase transitions. The transition from lamellar to nonlamellar phases could be facilitated by phospholipid synthesis in the presence of chemical activating agents. Subsequently, upon phospholipid breakdown, the system would revert back to the lamellar phase (Fig. 4A). We previously reported that the combination of the single-chain galactolipid *N*-oleyl β-D-galactopyranosylamine (GOA) and octylphenoxypolyethoxyethanol (IGEPAL) forms micrometer-sized spherical nonlamellar sponge phase droplets (*24*, *39*). Creating a 5 mM dispersion of GOA in HEPES buffer pH 8.0 containing 1.5 mM IGEPAL, results in formation of lipid sponge phase droplets (Fig. S14). However, when the same dispersion was formulated with the addition of 1.5 mM of lysophospholipid **1d** and oleic acid **2**, lamellar vesicles were observed and no sponge phase droplets were present (Fig. 4B). Differentiation between the lamellar lipid phase (vesicles) and nonlamellar sponge phase droplets was achieved through both phase contrast microscopy and monitoring the intensity profile of lipophilic dyes (*40*) (Fig. S17). Addition of HATU to trigger formation of phospholipid **3d** led to a striking transformation of the vesicles to lipid sponge phase droplets over 15 min (Fig. 4C). When **3d** was catabolized overnight at 37 °C, the droplets transitioned back to vesicles, illustrating that synthetic phospholipid metabolism can effectively regulate lipid phase transitions (Fig. S16).

A notable increase in assembly size was observed during the transition from lamellar phase vesicles to nonlamellar lipid sponge phase droplets. From the time-lapse microscopy, we attributed the size increase to fusion events that frequently occurred between individual droplets, similar to what has previously been observed (*24*, *25*). This observation prompted us to investigate whether

phospholipid metabolism could be utilized to trigger artificial cell fusion events and facilitate the interchange of membrane components between two initially separated lipid assemblies. Formation of phospholipid would convert lamellar vesicles to nonlamellar droplets, followed by fusion. Subsequently, lipid disassembly would lead to regeneration of the lamellar phase vesicles. If successful, this approach would offer a novel mechanism to induce membrane content mixing in artificial cells.

We prepared two samples of GOA vesicles in the presence of IGEPAL, **1d**, and **2**. Each vesicle population also contained 0.01 mol% of a phospholipid linked to a fluorescent dye, either DOPE-AlexaFluor488 or DOPE-Cy5. Upon combining the two samples, fluorescence microscopy images revealed that the vesicles maintained their membrane identity without undergoing fusion or fluorescent phospholipid exchange (Fig. 4D). However, 30 min after the addition of HATU, imaging revealed the presence of sponge phase droplets that contained both phospholipid dyes, confirming that membrane fusion and mixing had taken place (Fig. 4E). Following an overnight incubation at 37 °C during which phospholipid **3d** hydrolysis took place, the samples were examined again under fluorescence confocal microscopy. Sponge droplets had disappeared and were replaced with newly formed vesicles that contained both phospholipid dyes (Fig. 4F) demonstrating lipid interchange between distinct vesicle populations.

References and Notes

1. M. Edidin, Lipids on the Frontier: A Century of Cell-membrane Bilayers. *Nat. Rev. Mol. Cell Biol.* **4**, 414–418 (2003).

2. J. Lombard, Once Upon a Time the Cell Membranes: 175 Years of Cell Boundary Research. *Biol. Direct* **9**, 32 (2014).

3. R. Lipowsky, Remodeling of Membrane Compartments: Some Consequences of Membrane Fluidity. *Biol. Chem.* **395**, 253–274 (2014).

4. B. Wang, P. Tontonoz, Phospholipid Remodeling in Physiology and Disease. *Annu. Rev. Physiol.* **81**, 165–188 (2019).

5. H. Shindou, D. Hishikawa, T. Harayama, K. Yuki, T. Shimizu, Recent Progress on Acyl CoA: Lysophospholipid Acyltransferase Research. *J. Lipid Res.* **50**, S46–S51 (2009).

6. M. Murakami, I. Kudo, Phospholipase A2. *J. Biochem.* **131**, 285–292 (2002).

7. R. K. Grötsch, A. Angı, Y. G. Mideksa, C. Wanzke, M. Tena-Solsona, M. J. Feige, B. Rieger, J. Boekhoven, Dissipative Self-Assembly of Photoluminescent Silicon Nanocrystals. *Angew. Chem. Int. Ed.* **57**, 14608–14612 (2018).

8. R. K. Grötsch, C. Wanzke, M. Speckbacher, A. Angı, B. Rieger, J. Boekhoven, Pathway Dependence in the Fuel-Driven Dissipative Self-Assembly of Nanoparticles. *J. Am. Chem. Soc.* **141**, 9872–9878 (2019).

9. M. Tena-Solsona, J. Janssen, C. Wanzke, F. Schnitter, H. Park, B. Rieß, J. M. Gibbs, C. A. Weber, J. Boekhoven, Accelerated Ripening in Chemically Fueled Emulsions. *ChemSystemsChem* **3**, e2000034 (2021).

10. P. S. Schwarz, M. Tena-Solsona, K. Dai, J. Boekhoven, Carbodiimide-fueled Catalytic Reaction Cycles to Regulate Supramolecular Processes. *Chem. Commun.* **58**, 1284–1297 (2022).

11. G. W. Anderson, J. E. Zimmerman, F. M. Callahan, N-Hydroxysuccinimide Esters in Peptide Synthesis. *J. Am. Chem. Soc.* **85**, 3039–3039 (1963).

12. H. R. Hulett, Non-enzymatic Hydrolysis of Adenosine Phosphates. *Nature* **225**, 1248–1249 (1970).

13. F. Schnitter, A. M. Bergmann, B. Winkeljann, J. Rodon Fores, O. Lieleg, J. Boekhoven, Synthesis and Characterization of Chemically Fueled Supramolecular Materials Driven by Carbodiimide-based Fuels. *Nat. Protoc.* **16**, 3901–3932 (2021).

14. J. C. M. Holthuis, A. K. Menon, Lipid Landscapes and Pipelines in Membrane Homeostasis. *Nature* **510**, 48–57 (2014).

15. C. R. Kensil, E. A. Dennis, Alkaline Hydrolysis of Phospholipids in Model Membranes and the Dependence on their State of Aggregation. *Biochemistry* **20**, 6079–6085 (1981).

16. M. Tena-Solsona, C. Wanzke, B. Riess, A. R. Bausch, J. Boekhoven, Self-selection of Dissipative Assemblies Driven by Primitive Chemical Reaction Networks. *Nat. Commun.* **9**, 2044 (2018).

17. M. G. Howlett, R. J. H. Scanes, S. P. Fletcher, Selection Between Competing Self-Reproducing Lipids: Succession and Dynamic Activation. *JACS Au* **1**, 1355–1361 (2021).

18. C. Bonfio, C. Caumes, C. D. Duffy, B. H. Patel, C. Percivalle, M. Tsanakopoulou, J. D. Sutherland, Length-Selective Synthesis of Acylglycerol-Phosphates through Energy-Dissipative Cycling. *J. Am. Chem. Soc.* **141**, 3934–3939 (2019).

19. Z. A. Almsherqi, S. D. Kohlwein, Y. Deng, Cubic membranes: a legend beyond the Flatland of cell membrane organization. *J. Cell Biol.* **173**, 839–844 (2006).

20. R. Mezzenga, J. M. Seddon, C. J. Drummond, B. J. Boyd, G. E. Schröder-Turk, L. Sagalowicz, Nature-Inspired Design and Application of Lipidic Lyotropic Liquid Crystals. *Adv. Mater.* **31**, 1900818 (2019).

21. M. L. M. Jongsma, I. Berlin, J. Neefjes, On the Move: Organelle Dynamics during Mitosis. *Trends Cell Biol.* **25**, 112–124 (2015).

22. D. von Wettstein, Discovery of a Protein Required for Photosynthetic Membrane Assembly. *Proc. Natl. Acad. Sci. U.S.A.* **98**, 3633–3635 (2001).

23. D. Floris, W. Kühlbrandt, Molecular Landscape of Etioplast Inner Membranes in Higher Plants. *Nat. Plants* **7**, 514–523 (2021).

24. A. Bhattacharya, H. Niederholtmeyer, K. A. Podolsky, R. Bhattacharya, J.-J. Song, R. J. Brea, C.-H. Tsai, S. K. Sinha, N. K. Devaraj, Lipid Sponge Droplets as Programmable Synthetic Organelles. *Proc. Natl. Acad. Sci. U.S.A.* **117**, 18206–18215 (2020).

25. M. Moinpour, A. Fracassi, R. J. Brea, M. Salvador-Castell, S. Pandey, M. M. Edwards, S. Seifert, S. Joseph, S. K. Sinha, N. K. Devaraj, Controlling Protein Enrichment in Lipid Sponge Phase Droplets using SNAP-Tag Bioconjugation. *ChemBioChem* **23**, e202100624 (2022).

26. A. Fracassi, K. A. Podolsky, S. Pandey, C. Xu, J. Hutchings, S. Seifert, C. R. Baiz, S. K. Sinha, N. K. Devaraj, Characterizing the Self-Assembly Properties of Monoolein Lipid Isosteres. *J. Phys. Chem. B* **127**, 1771–1779 (2023).

27. T. Lu, E. Spruijt, Multiphase Complex Coacervate Droplets. *J. Am. Chem. Soc.* **142**, 2905–2914 (2020).

28. P. E. Saw, X. Xu, M. Zhang, S. Cao, O. C. Farokhzad, J. Wu, Nanostructure Engineering by Simple Tuning of Lipid Combinations. *Angew. Chem. Int. Ed.* **59**, 6249–6252 (2020).

29. L. S. Manni, W.-K. Fong, R. Mezzenga, Lipid-based Mesophases as Matrices for Nanoscale Reactions. *Nanoscale Horiz.* **5**, 914–927 (2020).

30. W. Sun, J. J. Vallooran, A. Zabara, R. Mezzenga, Controlling Enzymatic Activity and Kinetics in Swollen Mesophases by Physical Nano-confinement. *Nanoscale* **6**, 6853–6859 (2014).

31. S. Aleandri, R. Mezzenga, The Physics of Lipidic Mesophase Delivery Systems. *Phys. Today* **73**, 38–44 (2020).

32. A. S. Holehouse, R. V. Pappu, Functional Implications of Intracellular Phase Transitions. *Biochemistry* **57**, 2415–2423 (2018).

33. C. P. Brangwynne, P. Tompa, R. V. Pappu. Polymer Physics of Intracellular Phase Transitions. *Nat. Phys.* **11**, 899–904 (2015).

34. R. Rubio-Sánchez, D. K. O'Flaherty, A. Wang, F. Coscia, G. Petris, L. Di Michele, P. Cicuta, C. Bonfio, Thermally Driven Membrane Phase Transitions Enable Content Reshuffling in Primitive Cells. *J. Am. Chem. Soc.* **143**, 16589–16598 (2021).

35. C. Donau, F. Späth, M. Stasi, A. M. Bergmann, J. Boekhoven, Phase Transitions in Chemically Fueled, Multiphase Complex Coacervate Droplets. *Angew. Chem. Int. Ed.* **134**, e202211905 (2022).

36. P. L. Yeagle, F. T. Smith, J. E. Young, T. D. Flanagan, Inhibition of Membrane Fusion by Lysophosphatidylcholine. *Biochemistry* **33**, 1820–1827 (1994).

37. L. Chernomordik, A. Chanturiya, J. Green, J. Zimmerberg, The Hemifusion Intermediate and its Conversion to Complete Fusion: Regulation by Membrane Composition. *Biophys. J.* **69**, 922–929 (1995).

38. N. Fuller, R. P. Rand, The Influence of Lysolipids on the Spontaneous Curvature and Bending Elasticity of Phospholipid Membranes. *Biophys. J.* **81**, 243–254 (2001).

39. C. Xu, A. Fracassi, C. P. Baryiames, A. Bhattacharya, N. K. Devaraj, C. R. Baiz, Sponge-phase Lipid Droplets as Synthetic Organelles: An Ultrafast Study of Hydrogen Bonding and Interfacial Environments. *ChemPhysChem* **24**, e202300404 (2023).

40. T. Imura, H. Yanagishita, D. Kitamoto, Coacervate Formation from Natural Glycolipid: One Acetyl Group on the Headgroup Triggers Coacervate-to-Vesicle Transition. *J. Am. Chem. Soc.* **126**, 10804–10805 (2004).

Acknowledgments: The authors acknowledge the facilities along with the scientific and technical assistance of the staff of the cryoEM facility at UC San Diego. Dr. Kira A. Podolsky is acknowledged for her valuable contribution to preparing the figures. **Funding:** This work was funded by the National Science Foundation (CHE-2304664) and the Agencia Estatal de Investigación (AEI) and the Ministerio de Ciencia e Innovación (MICINN) [PID2021-128113NA-I00]. RJB also thanks the Agencia Estatal de Investigación (AEI) and the Ministerio de Ciencia e Innovación (MICINN) for his Ramón y Cajal contract (RYC2020-030065-I). **Author contributions:** AF, AS, RJB, and NKD conceived the idea. AF, AS, and RJB carried out the synthesis of the organic molecules, the characterization of the lipid assemblies, and all the experiments presented in the manuscript. AF, AS, RJB, and NKD analyzed and interpreted the results. AF, AS, RJB, and NKD wrote and reviewed the manuscript. **Competing interests:** Authors declare that they have no competing interests. **Data and materials availability:** All the synthetic procedures, methodologies, and data reported in this manuscript are available in the main text or the supplementary materials.

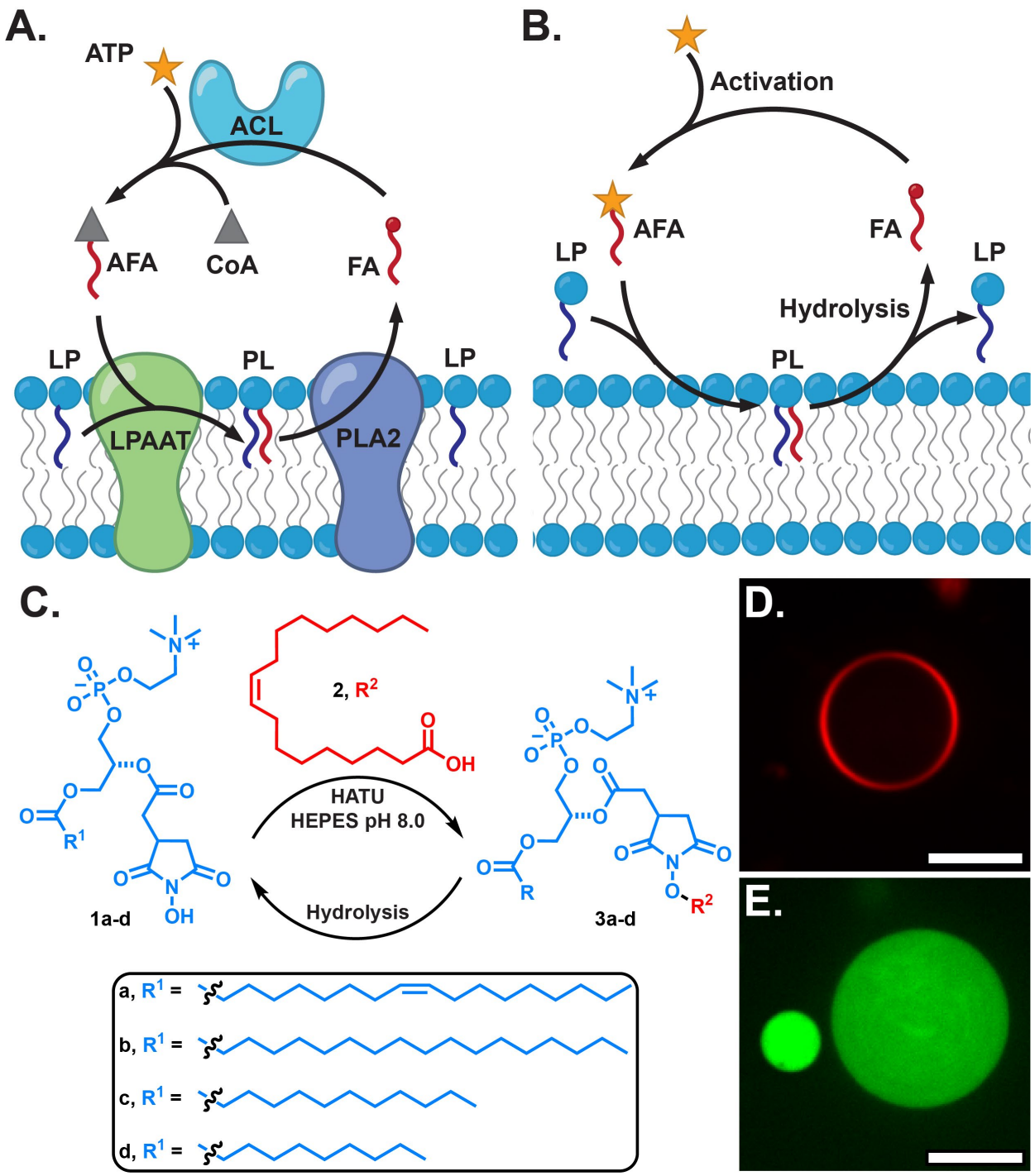

Fig. 1. Establishing an abiotic phospholipid metabolic network. (**A**) Representative illustration of a typical enzymatic metabolic cycle for native phospholipids within a biological system. Fatty acids (FA) are converted to activated fatty acids (AFA) by acyl-coenzyme A ligase (ACL) using coenzyme A (CoA) and adenosine triphosphate (ATP). AFAs are then utilized by lysophosphatidic acid acyl transferase (LPAAT) to catalyze the transfer of an acyl chain onto a lysophospholipid (LP), resulting in the synthesis of a phospholipid (PL). Phospholipase A2 (PLA2) then catalyzes the breakdown of PL to regenerate the precursors LP and FA. (**B**) Proposed abiotic phospholipid metabolism. The process begins with the activation of FAs at the expense of chemical energy

emulating the function of ATP in biological systems to generate AFAs. AFAs then spontaneously couple with lysophospholipid (LP) to generate a phospholipid (PL). The chemical linkage formed is transient and PL hydrolyzes over time regenerating the precursors LP and FA. (**C**) Reaction scheme for the synthesis of phospholipid **3a-d** by coupling of the NHS-lysophospholipid **1a-d** with oleic acid **2**. The NHS-ester formed is unstable at pH 8.0 and slowly hydrolyzes over time to regenerate the precursors **1a-d** and **2**. (**D**) Fluorescence microscopy images of phospholipid **3a** vesicles stained with 0.01 mol% Texas-Red DHPE obtained by gentle rehydration in HEPES buffer pH 8.0. Scale bars denote 10 µm. (**E**) Fluorescence microscopy images of phospholipid **3a** vesicles obtained by gentle rehydration in HEPES buffer pH 8.0 showing encapsulation of the polar dye HPTS in the aqueous core. Scale bars denote 10 µm.

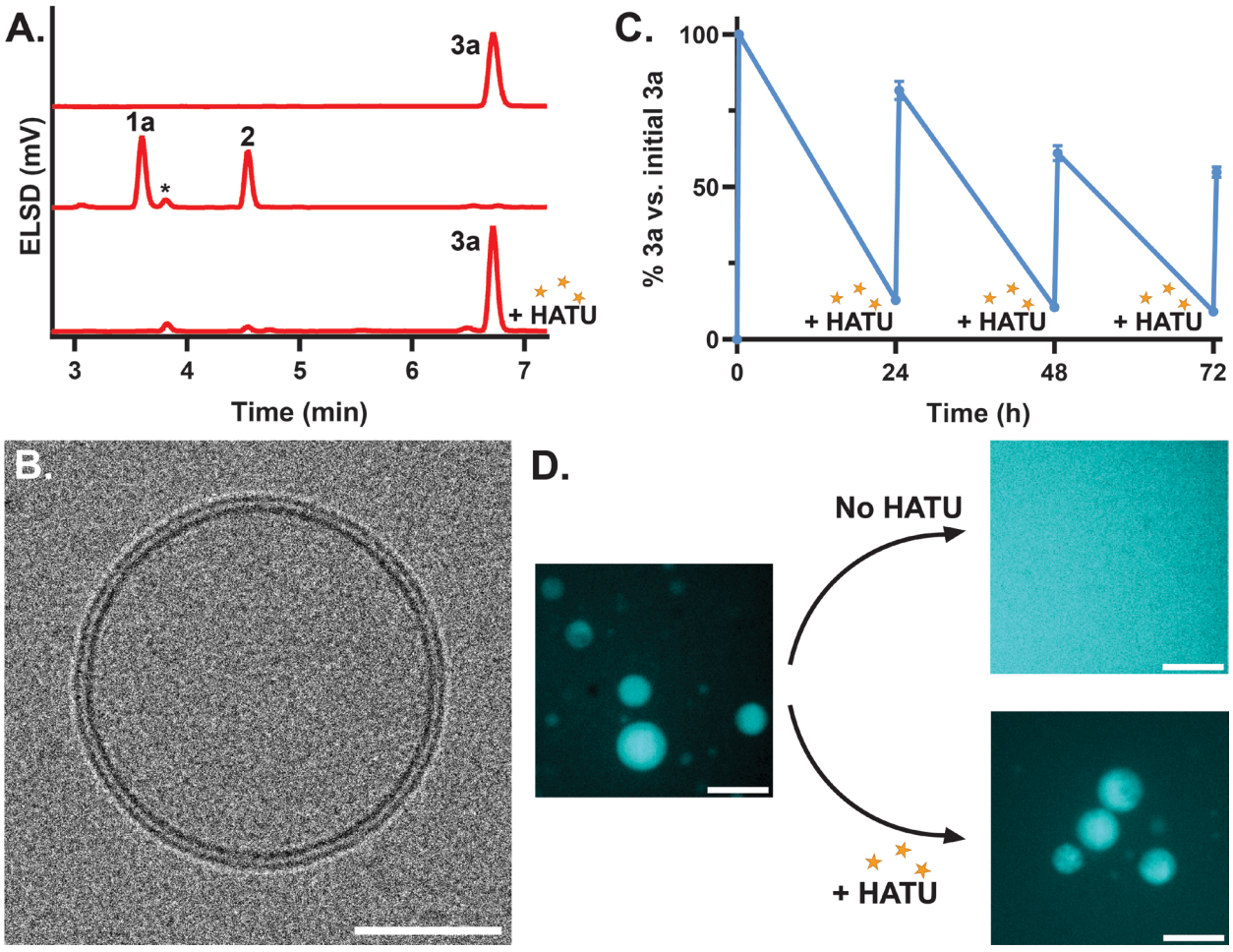

Fig. 2. Characterization of the synthetic phospholipid metabolic network. (**A**) HPLC-ELSD traces of a 1.25 mM dispersion of phospholipid **3a** in HEPES buffer pH 8.0 before hydrolysis (*top*), after 24 h incubation at 37 °C to generate lysophospholipid **1** and oleic acid **2** (*middle*), and 15 min after the addition of 1 equivalent of HATU (*bottom*) showing full conversion back to phospholipid **3a**. The formation of the Lyso $C_{18:1}$ PC hydrolysis side product is indicated with an asterisk (*). (**B**) A representative cryoEM image of a vesicle formed during the in situ synthesis of phospholipid **3a** confirming the presence of a phospholipid bilayer structure. Scale bar denotes 50 nm. (**C**) Consecutive rounds of formation and hydrolysis of phospholipid **3a**. For each cycle, 1

equivalent of HATU was administered, followed by a 24 h incubation at 37 °C. Error bars represent standard deviation (n = 3). (**D**) Fluorescence microscopy images of phospholipid **3a** vesicles in HEPES buffer pH 8.0, encapsulating the Cy5 fluorescent probe (*left*). After 24 h incubation at 37 °C, Cy5 is released to the environment in the absence of HATU (*top right*). Addition of 1 equivalent of HATU maintains the metabolic network and preserves structural integrity of the synthetic phospholipid membrane and the retention of dye within vesicles (*bottom right*). The scale bar indicates 10 µm.

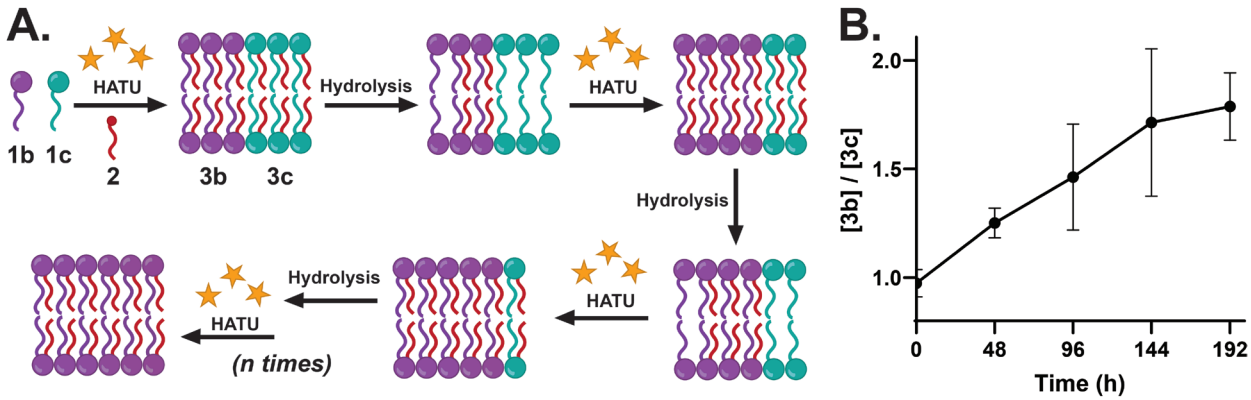

Fig. 3. Enrichment of specific phospholipids during synthetic metabolism. (**A**) Schematic representation of the phospholipid metabolic cycles [LPs: lysophospholipids, FA: fatty acid]. The metabolic cycles involve the synthesis and hydrolysis of two phospholipids with different hydrolytic rates, showing gradual accumulation of phospholipids with slower hydrolytic rates within the membrane after repeated cycles. (**B**) Analysis of the [**3b**]/[**3c**] phospholipid ratio as it evolves over several metabolic cycles. For each cycle, 1 equivalent of HATU based on the available oleic acid **2** was administered, followed by a 48 h incubation at 25 °C. Error bars represent standard deviation (n = 3).

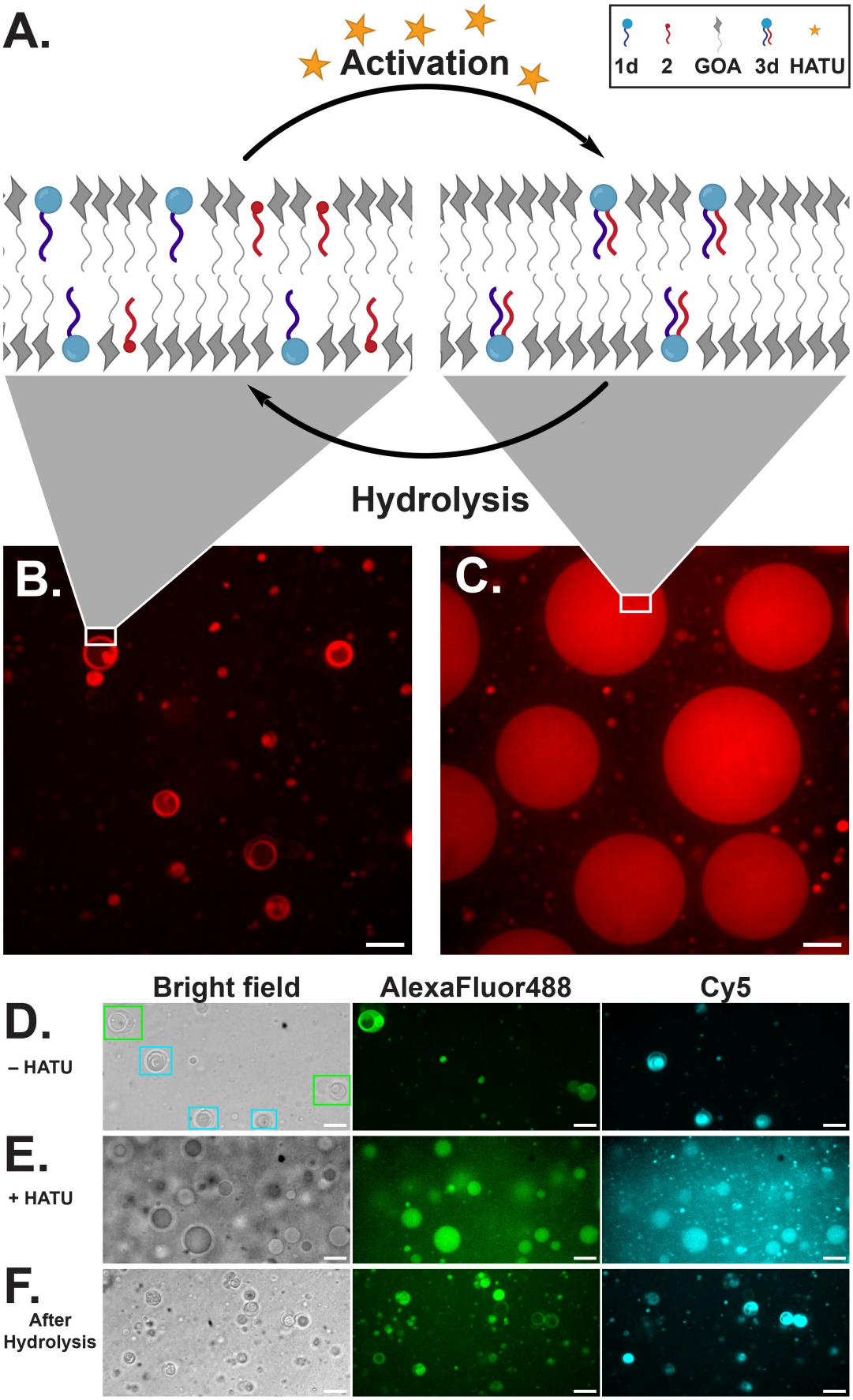

Fig. 4. Membrane phase transitions governed by a phospholipid metabolic network. (**A**) Schematic representation of the proposed lipid phase transition regulated through a phospholipid metabolic cycle [LP: lysophospholipid, FA: fatty acid, GOA: *N*-oleyl β-$_D$-galactopyranosylamine lipid, PL: phospholipid]. The presence of the single-chain amphiphiles LP and FA in the lipid mixture determines the formation of lamellar phase assemblies (vesicles). PL synthesis, triggered by a chemical activating agent, triggers the transition from vesicles to the nonlamellar sponge phase lipid droplets. Conversely, PL hydrolysis regenerates LP and FA leading to the transition back to the lamellar phase. (**B**) Fluorescence microscopy image of vesicles obtained by rehydrating a mixture of GOA (5 mM), lysophospholipid **1d** (1.5 mM), oleic acid **2** (1.5 mM), and Texas Red-DHPE (0.01 mol%) with a solution of IGEPAL (1.5 mM) in HEPES buffer pH 8.0. Scale bar denotes 10 µm. (**C**) Fluorescence microscopy image of sponge phase droplets obtained by adding 1 equivalent of HATU to a dispersion of GOA (5mM), lysophospholipid **1d** (1.5 mM), oleic acid **2** (1.5 mM), Texas Red-DHPE (0.01 mol%), IGEPAL (1.5 mM) in HEPES buffer pH 8.0. Scale bar denotes 10 µm. (**D**) Fluorescence microscopy images of vesicles obtained by mixing two samples of GOA vesicles prepared as in Fig. 4B, stained with DOPE-AlexaFluor488 (0.01 mol%) and DOPE-Cy5 (0.01 mol%), respectively. Green boxes in the bright field highlight vesicles labeled with DOPE-AlexaFluor488 while cyan boxes highlight vesicles labeled with DOPE-Cy5. Scale bar denotes 10 µm. (**E**) Fluorescence microscopy images of sponge phase droplets obtained adding 1 equivalent of HATU to the vesicles described in Fig. 4D. After the lipid phase transition, all the droplets contain both dyes, indicating lipid mixing has taken place due to droplet fusion. Scale bar denotes 10 µm. (**F**) Fluorescence microscopy images of vesicles obtained after incubating the sponge phase droplets described in Fig. 4E at 37 °C, overnight. All the newly generated vesicles contain both dyes, indicating lipid exchange. Scale bar denotes 10 µm.